Trends in Analytical Chemistry 140 (2021) 116241

Contents lists available at ScienceDirect

Trends in Analytical Chemistry

journal homepage: www.elsevier.com/locate/trac

Nonlinear optical characterization of pharmaceutical formulations

Alex M. Sherman [a, 1], Nita Takanti [a, 1], Jiayue Rong [a], Garth J. Simpson [a, *]

[a] Department of Chemistry, Purdue University, 560 Oval Drive, West Lafayette, Indiana 47907, United States

ARTICLE INFO

Article history:
Available online 13 March 2021

Keywords:
Nonlinear optics
Active pharmaceutical ingredients
Pharmaceuticals
Second harmonic generation
Stimulated Raman spectroscopy
Coherent anti-Stokes Raman spectroscopy
Polymorphism
Amorphous solid dispersions
Dissolution
Differential scanning calorimetry

ABSTRACT

Unique challenges in formulating the next generation of active pharmaceutical ingredients (APIs) into stable formulations demand analytical tools not currently available using common benchtop methods. Herein, we review approaches to address some of these challenges through leveraging nonlinear optical (NLO) interactions between light and matter. Applications in dissolution testing, polymorphism, and accelerated stability testing highlight the breadth of these methods. The specificity of second harmonic generation (SHG) to chiral crystals supports rapid polymorphism analysis at the limit of individual crystals and informs formulations designs to address solubility challenges common in emerging drug candidates. Coherent anti-Stokes Raman spectroscopy (CARS) and stimulated Raman spectroscopy (SRS) provide vibration-specific microscopy of final dosage forms to inform composition at video-rate acquisition speeds and ~1 μm spatial resolution. Recent results are reviewed to illustrate challenges in designing formulations for emerging drug candidates and opportunities for the development of NLO tools tailored to meet them.

© 2021 Elsevier B.V. All rights reserved.

1. Introduction

The complexity of small molecule active pharmaceutical ingredients (APIs) and drug delivery systems (DDSs) has progressively increased throughout the 21st century, driving corresponding needs for measurement innovations to ensure delivery of safe and effective final dosage forms. Strict regulations about drug and device development have increased in parallel – pharmaceutical products that reached the marketplace are subject to extensive research and product safety protocols to achieve approval for broad use. Currently, the FDA has set processes and regulations in place throughout the development pipeline, spanning initial conception and demonstration of therapeutic molecules to pre-clinical testing to complex clinical trials in humans. In 2014, this process cost up to 1.3 billion US dollars, with only 1 in 1000 potential drug candidates making it to human clinical trials in the US (after which, 10% still fail) [1]. Formulation development impacts this pipeline by dictating stability and bioavailability. The 'Target Product Quality Profile' (TPQP) helps to guide formulations design by defining core quality characteristics of the drug for safety and efficacy [2]. Many physical and chemical properties of the drug substance impact the TPQP. Physical properties of the drug encompass polymorphism and aqueous solubility of the API. Chemical properties include the chemical stability in solid state and solution [3]. Since these biopharmaceutical characteristics are critical to the TPQP, there is a growing need for technologies capable of rapidly and accurately informing on physical and chemical critical quality attributes for increasingly complex APIs and formulations.

In this review, we will be identifying major barriers currently throttling formulations design and critically assessing the strengths and limitations of NLO techniques for providing sensitive and rapid analyses to assess the TPQP of an API. NLO techniques often provide chemical specificity, high signal-to-noise ratios (SNR), low limits of detection, nondestructive analyses, and short acquisition times [4]. The review will discuss NLO application in screening crystallization conditions for new crystal forms, assessing stability in amorphous solid dispersions (ASDs), measuring dissolution kinetics and phase behavior, and probing API dissolution kinetics in biorelevant media.

2. Background of NLO techniques

A brief overview of the most common coherent nonlinear optical interactions is presented in order to provide a foundation for interpreting the unique information content accessible through NLO measurements. For more detailed explanations of

* Corresponding author.
E-mail address: gsimpson@purdue.edu (G.J. Simpson).
[1] These authors contributed equally to this work.

https://doi.org/10.1016/j.trac.2021.116241
0165-9936/© 2021 Elsevier B.V. All rights reserved.

nonlinear optics in biology and chemistry, readers are encouraged to seek out further supporting information [5,6]. In general, NLO describe coherent optical processes scaling nonlinearly with the incident light intensity, such that they are most significant in intense optical fields (e.g., as arising in the focus of an ultrafast laser pulse). Ultrashort laser pulses, with durations from picosecond to femtosecond, support the high peak powers for efficient NLO processes while maintaining low average power to minimize perturbations from local heating. In beam-scanning microscopy configurations, the nonlinear scaling with laser power localizes NLO processes to the focal volume, providing "confocal" sectioning capability and reducing out-of-focus background contributions.

Second harmonic generation (SHG) is arguably among the simplest nonlinear optical processes, in which the frequency of light is doubled after interaction with a material (shown in Fig. 1). Classically, SHG can be intuited by considering "sloshing" of electrons within a molecule in response to a driving optical field. The corresponding induced polarization within the material can re-radiate. In linear optics, this re-radiation describes scattering for isolated particles and reflection/refraction for bulk media. When the optical field is sufficiently high (e.g., upon focusing an ultrafast laser pulse), the anharmonic regions of the potential energy surface can be accessed. Classical resonant motion along an anharmonic potential driven at the resonant frequency ω contains contributions not only at the harmonic frequency ω, but also at higher harmonics [5]. These same anharmonic effects can result in frequency-mixing when driven by multiple incident fields. From classical considerations of symmetry, even harmonics (2ω, 4ω, etc.) are forbidden in centrosymmetric and isotropic bulk media, providing selectivity for materials ordered into noncentrosymmetric assemblies [5]. For the nondegenerate case, in which the incoming fields are of different frequency, three-wave mixing to produce sum ($\omega_1 + \omega_2 = \omega_{sum}$) or difference ($\omega_1 - \omega_2 = \omega_{diff}$) frequency generation (SFG or DFG, respectively) shares much of the same symmetry-selectivity as SHG, as SHG is just a specific instance of SFG with degenerate incident frequencies. In contrast, four-wave mixing underpinning CARS and SRS is bulk-allowed in isotropic media, with selectivity arising from vibrational resonances. Thus, three and four wave mixing processes are highly complementary. This classical description based on anharmonicity within the molecular polarizability does not capture the subtleties of descriptions that properly integrate quantum mechanical resonances [7] (e.g., derived from perturbation theory [8]), but nevertheless provides a comparatively simple qualitative framework for understanding some of the key symmetry-related attributes of nonlinear optical processes applied to pharmaceutical materials analysis.

When considering specific applications of nonlinear optics for pharmaceutical materials analysis, the non-centrosymmetry requirement of SHG/SFG is particularly noteworthy. Most new small-molecule drug candidates are homochiral [9], and therefore necessarily non-centrosymmetric at the molecular level. Although a solution of chiral solutes is also non-centrosymmetric, coherent SHG is still symmetry-forbidden in isotropic, disordered assemblies. However, no ordered assembly of homochiral molecules can be centrosymmetric, with homochiral molecules necessarily adopting non-centrosymmetric lattices upon crystallization. With the exception of a few relatively rare high-symmetry space groups, these accessible space groups for homochiral molecules are symmetry-allowed for coherent SHG, while disordered aggregates, liquids, or solubilized forms of these same molecular species are not. The background suppression imposed by this symmetry selectivity provides high crystal-specificity in second order nonlinear optical imaging of chiral crystals (SONICC) [10].

Driven in part by the high sensitivity of SHG to molecular ordering, the polarization-dependence of nonlinear optics is richer than in linear optics, with polarization modulation of the incoming light greatly increasing the information content relative to measurements of the intensity alone [5,11,12]. In previous studies, SHG polarization analysis has supported discrimination of crystal polymorphs with high statistical confidence, short analysis timeframes, and low sample requirements compatible with high-throughput crystal form screening [11,12]. This dependence is related to the second order susceptibility tensor ($\chi^{(2)}$) of a material, which dictates how the material interacts with electric field components describing a given polarized field. Polarization analysis in SHG measurements, can enable recovery of the unique elements of the $\chi^{(2)}$ tensor, which in turn are highly dependent on structure and orientation. Polarization modulation can be performed by multiple methods such as introduction simple waveplates and polarizers [11–13]. Improvements in signal to noise through suppression of 1/f noise can be realized by rapid modulation using an electrooptic modulator (EOM) [13]. Alternatively, rapid modulation for SNR enhancement can also be achieved through spatial modulation of polarization using a microretarder array [14]. These polarization-dependent measurements can significantly increase the

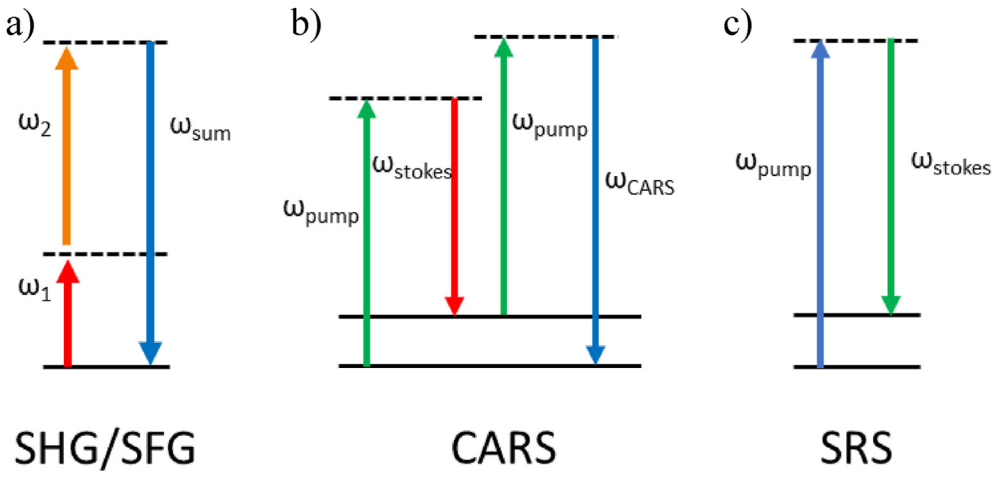

Fig. 1. Jablonski diagrams for commonly used nonlinear optical techniques: a) sum frequency generation (SFG) which converges to second harmonic generation (SHG) when $\omega_1 = \omega_2$, b) coherent anti-Stokes Raman scattering (CARS), and c) stimulated Raman scattering (SRS).

information content of SHG analyses relative to simple measurements of intensity alone.

Information content can also be increased by higher-order nonlinear optical interactions. Coherent anti-Stokes Raman scattering (CARS) is a nonlinear process in which commonly two beams of light interact with a material to probe the vibrational motion of molecules (shown in Fig. 1b) [5,6]. This process, known as four-wave mixing, produces an anti-Stokes shifted beam of light with frequency (ω_{CARS}) equal to $2\omega_{pump} - \omega_{Stokes}$. By tuning the frequency difference between the pump (ω_{pump}) and Stokes beams (ω_{Stokes}) to match the frequency of a vibrational energy transition, coherence is established between the ground and vibrational excited states. This coherence is then interrogated by another interaction with the pump beam to produce four-wave mixing at the anti-Stokes shifted frequency, with the corresponding blue-shifted beam isolated by spectral filtering. The efficiency of this four-wave mixing process is greatly increasing by the presence of a vibrational resonance, enabling coherent spectroscopy of vibrational transitions. The frequency difference between pump and Stokes beams can be tuned to experimentally acquire a CARS spectrum informing on the vibrational motions of the sample. In CARS microscopy, the pump and Stokes beams are typically co-propagated and scanned across the field-of-view (FoV). The pump or Stokes frequency (or time-delay tuning in chirped-pulse CARS) can then be swept to perform spectroscopy, enabling chemical selectivity based on Raman spectral differences. Four-wave mixing with a different arrangement of interactions (pump and pump, followed by Stokes and CARS) can also produce a coherent signal from interactions with electronic states, contributing to a non-resonant background that can interfere coherently with the vibrational resonances in CARS and alter spectral peak-shapes, frustrating simple spectral decomposition approaches.

Stimulated Raman scattering (SRS) is another NLO technique (shown in Fig. 1) for probing the molecular vibrations of a sample without significant interferences from non-resonant contributions [5,6]. Like CARS, a sample interacts with a pump and Stokes beam and the frequency difference between the two beams is tuned to resonance with a vibrational transition. Unlike CARS, SRS arises from population transfer, resulting in a small fraction of power interchanging between pump and Stokes beams after interaction with the sample. Whereas CARS scales with the squared magnitude of the complex nonlinear susceptibility, SRS probes only the imaginary part describing losses associated with the population transfer event. This energy change is then measured by stimulated Raman gain (SRG) of the Stokes beam, or by stimulated Raman loss (SRL) of the pump beam. Due to the magnitude of SRG and SRL commonly being orders of magnitude smaller than the pump and Stokes signals, high frequency modulation of one or both input beams is often performed with lock-in amplification for signal amplification. Unlike CARS, SRS is free coherent interference with the non-resonant (real-valued) background. In this review, applications of both SRS and CARS for pharmaceutical materials analysis will be discussed.

3. Polymorphism and crystal/physical form analysis

In solid-state formulations, the crystal form of an API can profoundly impact chemical stability, bioavailability, and toxicity [15–17]. The impact of crystal form on bioavailability is arguably best illustrated in the high profile case of ritonavir, which is an antiretroviral medication for the treatment of HIV/AIDS [18]. The original formulation was recalled and reformulated after a new crystal form for ritonavir appeared (Form II) with much lower solubility and bioavailability than the originally identified Form I. The recall and reformulation significantly delayed delivery to those in need and exacted significant direct and indirect costs to the manufacturer. Consequently, intellectual property rights for APIs generally include identification of the suite of accessible physical forms in addition to chemical composition [19]. Likewise, extensive exploration is routinely performed to characterize the polymorphic pathways affecting the physical and chemical conditions of APIs in the solid state. Common benchtop methods for interrogating crystal form include structural analysis [powder X-ray diffraction (pXRD)], thermal analysis [differential scanning calorimetry (DSC), thermogravimetric analysis (TGA)], and spectroscopic analysis [Raman, Fourier-transform infrared (FTIR), nuclear magnetic resonance (NMR), terahertz (THz) Raman] [20–24].

Trends toward high-throughput screening and early stage characterization with limited API availability are collectively straining the capabilities of these established measurement approaches [25]. At later stages in formulations design, for which abundant API material is available, a myriad of sample conditions are regularly tested to identify new polymorphs and crystal forms and assess physical/chemical stability [26,27]. Increasing the scope of conditions assayed helps to improve the confidence in identification of most readily available stable crystal forms, but can slow development if analyses have long required measurement and growth times. For the speed of many of these methods, commonly integration times of 30–60 s or longer are needed in order to determine the solid state form [25], frustrating integration into high-throughput pipelines. As crystal form analyses are pushed to earlier stage development, an increasing number of potentially viable small molecule candidates may be considered with limited material availability for each, further exacerbating high-throughput integration [25,26]. Methods such as pXRD or DSC require relatively large sample volumes (several mg), throttling the number of conditions that can be tested in material-limited analyses. Therefore, methods capable of decreases in analysis times and/or reductions in sample size have the potential to propel drug crystal form screening by directly addressing critical bottlenecks in these early-stage investigations.

In this context, optical microscopy has several desirable properties for high-throughput particle identification and characterization of new crystal forms [28,29]. In the simplest applications, characterization is done by means of bright-field (BF) illumination or other linear microscopy methods (fluorescence, absorbance, scattering) and the physical form is qualitatively decided from these images [28,29]. Characterization based on microscopy likewise gives access to the unique crystal habit information content inaccessible with conventional techniques such as DSC or TGA [30,31]. While DSC and TGA are a widely-used techniques for polymorphic determination, most thermal analysis techniques rely on ensemble measurements that obscure single-particle transformations [30]. Particle-to-particle differences are particularly relevant to polymorph determination where in ensemble-averaged results may obscure low-abundance unique crystal forms arising stochastically within the sample. Contrasting these ensemble-averaged methods, physical and chemical changes to individual crystals can be observed by microscopy techniques with sufficient imaging resolution [29,30]. Thus, heterogeneous interactions of a material and changes in physical form on a per-particle basis overlooked by thermal analysis techniques are potentially accessible in microscopy measurements. Unfortunately, gross morphology of crystal habit accessible by bright-field and cross-polarized imaging is not necessarily uniquely linked to crystal form, with one crystal form often capable of presenting multiple habits.

Recent developments in nonlinear optics greatly extend the capabilities of optical imaging to target these bottlenecks in polymorphism and crystalline/physical form characterization [11,30,32–47]. Relative to bright-field and polarized (linear) microscopy, nonlinear optical microscopy can significantly increase the information content of the measurements, allowing for improvements in the confidence of polymorph determination [11,12]. Nonlinear optical interactions are highly sensitive to local structure within the material under interrogation [11]. This sensitivity is particularly poignant in second order nonlinear optical interactions by nature of the symmetry requirements for SHG and SFG. Microscopically disordered systems are symmetry-forbidden for coherent SHG. However, the vast majority of crystals produced by homochiral molecules adopt space groups that are bulk-allowed for coherent SHG. Thus, slight changes in the structure of a sample can significantly affect both the magnitude and polarization-dependence of the nonlinear optical conversion process to generate SHG [11,30]. Therefore, SHG microscopy, and other NLO techniques with similar structural symmetry requirements, can be used to add structural information to microscopy methods when evaluating physical forms of individual crystalline particles. Second harmonic generation imaging can be performed at up to kHz frame rates with high symmetry-selectivity for homochiral crystals [30,38,48]. Limits of detection of a few ppm are routinely realized nondestructively in volumes of only a few μg of material. Nonlinear optical processes provide several complementary approaches for crystal form analysis, representative examples of which are highlighted herein: spatial information by NLO microscopy [21,30], spectral characterization by NLO spectroscopy [38], and polarization analysis by NLO Stokes ellipsometry [11–13].

Recent studies by Sherman et al. shown in Fig. 2 illustrate the advantage of “hyphenated” measurements, in which NLO microscopy guides targeted independent analysis methods (in this case, thermal analysis for improved polymorph determination) [30]. Specifically, this work focused on improving DSC, which is commonly used in the drug discovery pipeline as a method of mapping the polymorphic pathways of a material with respect to changes in temperature. For ASDs and other pharmaceutical materials, temperature-dependent structural phase transitions in the API and/or the polymer host matrix can dramatically affect stability and bioavailability [17,34]. Conventional DSC relies on ensemble-averaged measurements that overlook subtle, heterogeneous changes in crystalline form, since the thermal response of individual microcrystals is generally well below the limit-of-detection of DSC. Each isolated particle can potentially undergo multiple unique phase transformations, driven by stochastics associated with the nucleation of new phases during temperature cycling. Fig. 2a shows such behavior for the dehydration of trehalose dihydrate in which Sherman et al. observed individual particles undergoing distinctly different dehydration pathways. A diversity of onset-times is observed for transition to a dehydrated form with greater SHG activity. This potentially rich diversity in phase behavior is inaccessible by ensemble-averaging over many particles in DSC measurements.

To overcome this absence of per-particle sensitivity of DSC while retaining the information content from thermal analysis, SHG microscopy was performed concurrently with DSC [30]. As shown in Fig. 2b, combined DSC and SHG measurements were performed on urea as proof of concept. SHG activity of individual urea microcrystals was shown to stochastically and rapidly drop to zero (vertical lines) as each particle in the FOV was seen to melt throughout the melting peak of the DSC trace (black line). Fig. 2c shows SHG images collected during this melting transition.

Following these proof-of-concept studies of a simple melting transition, SHG-DSC was used to investigate the more complex phase transitions of trehalose undergoing structural reorganization upon dehydration, providing evidence of a short-lived “cold phase transformation”, shown in Fig. 2a [30]. Analogous to reports of “cold crystallization” in DSC, increases in temperature produce increases molecular diffusion, which in turn provides the kinetic driver for thermodynamically favored phase transitions. Evidence for cold phase transformation in Fig. 2a is indicated by the sharp increase in SHG activity in each particle prior to the melting transition at ~230 °C. Unlike cold crystallization, in which kinetically trapped assemblies crystallize upon heating, the cold phase transformation in this study transitioned from one crystalline solid-state phase to another upon heating [49]. The crystalline form produced was short-lived, rapidly undergoing subsequent transition to a melted phase. The transient nature of the intermediate state was significantly shorter than the DSC response time, resulting in a single endothermic peak completely obscuring the transient crystal form observable by integration with SHG microscopy.

In molecular crystals, THz spectroscopic region provides insights into low-frequency librational motions, such as the rocking of intact molecules within a lattice. THz spectra tend to produce broad features in disordered media from inhomogeneous broadening, but periodicity within a molecular crystal generally results in sharp features that depend sensitively on molecular arrangement within the lattice. THz spectroscopy can be performed through direct absorption of THz radiation, through nonlinear optical interactions such as Kerr-effect spectroscopy [50], through inelastic neutron scattering [51], and through both spontaneous and coherent/stimulated Raman spectroscopy. Knowledge of the solid-state properties is one of the key issues in understanding the performance of drugs, and terahertz pulsed imaging has been shown to be effective for discrimination and quantification of polymorphs/hydrates, analysis of solid form transformation dynamics, quantitative characterization of tablets and tablet coatings [15–17]. The long wavelengths associated with direct absorption measurements of THz radiation are less prone to scattering, enabling much longer penetration depths than methods using visible light. In contrast to spontaneous THz Raman, coherent anti-Stokes Raman spectroscopy (CARS) has two additional advantages: i) CARS scales nonlinearly with peak intensity, such that negligible background is generated outside the focal volume, and ii) CARS interrogates a smaller, targeted spectral window relative to spontaneous Raman, providing a signal to noise advantage within this window [39,41,52]. Single beam THz-CARS microscopy can extend librational regions beyond the lower limit of ~600 cm^{-1} in conventional CARS to as low as 20 cm^{-1} with 14 cm^{-1} spectral resolution [52]. Other work based on linear and nonlinear THz spectroscopy have been reported on crystalline material identification, drug polymorph and hydrate form identification, and degree of crystallinity [39–41]. For example, THz-CARS has been used to non-destructively and non-invasively measure the porosity of pharmaceutical tablets, with multiple studies investigating different, complex formulation and shapes. In addition, the THz-CARS technique has the ability to probe isolated pores in the core of the matrix, which is usually challenging to detect by conventional porosimetry methods that rely on assessing the pores from the outside [39–42]. By enabling access to this structure-rich low-frequency vibrational and librational regime, THz-CARS and THz-SRS techniques are finding growing acceptance within the pharmaceutical community.

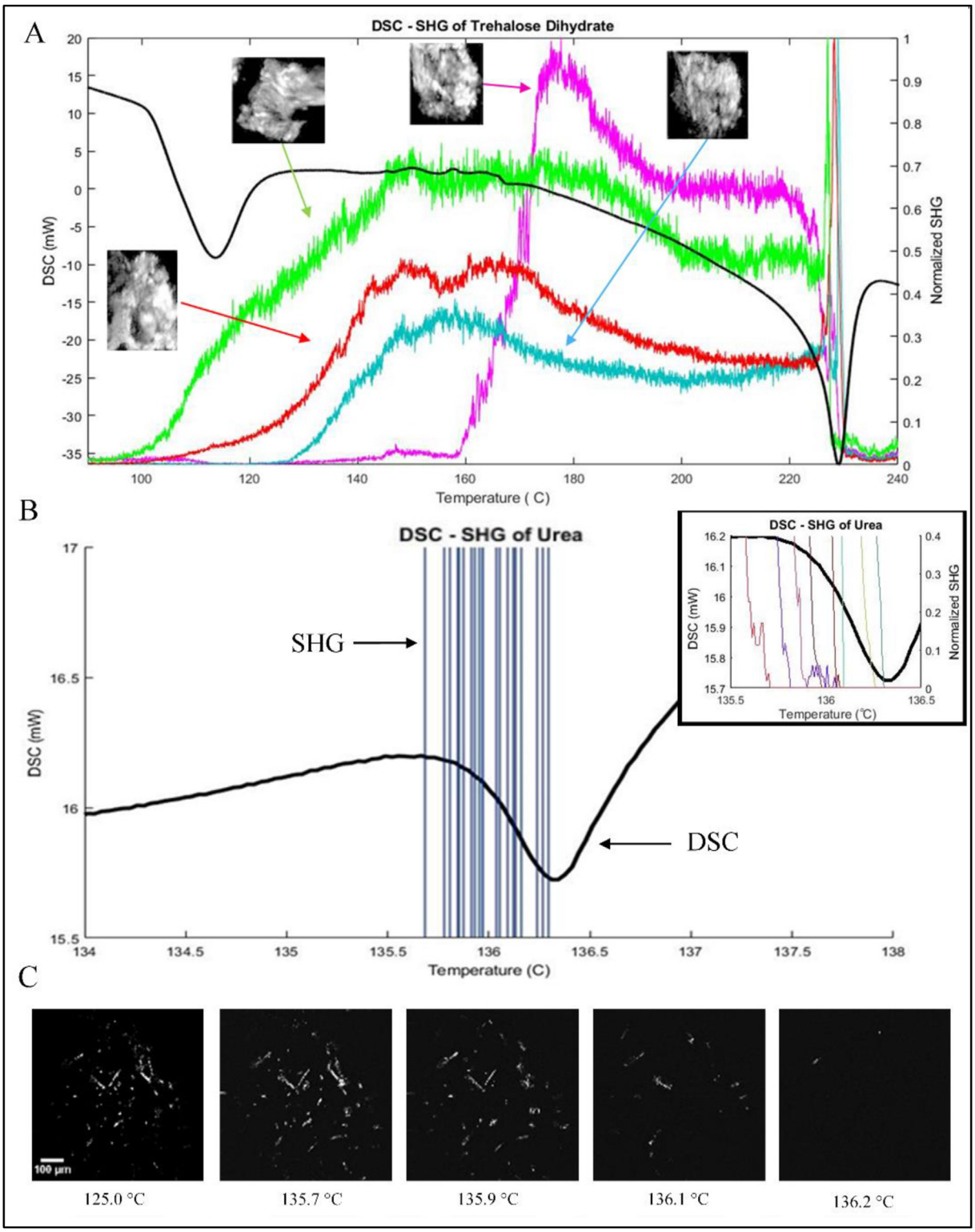

Fig. 2. (A) SHG/DSC analysis of trehalose by SHG microscopy. The multi-colored lines show the percentage of pixels of the trehalose particles above an SHG intensity threshold. These multi-colored lines are overlaid with the black line of the DSC trace, with endothermic direction being down (left axis). SHG/DSC images were summed for the temperature range of 140–220°C. The logarithm of the summed image was cropped to the measured region of each particle. The insets are the cropped images, pointing to their respective SHG trace. (B) The figure shows combined SHG microscopy with DSC analysis of urea. The melting trace of urea is shown by the solid black line of the DSC trace. As SHG was collected with the DCS data, the temperatures in which the normalized SHG intensity of individual urea particles drops below a value of 10% is shown by the vertical colored lines. DSC and SHG measurements running concurrently both indicate, within the same temperature range, a structural change. The inset shows a zoom-in of the temperature range 135.5–136.5°C where the color lines correspond to the normalized SHG intensity of urea. (C) SHG microscopy images of urea crystals during the analysis. SHG microscopy allows us to do analysis on a per-particle basis while also revealing the stochastic nature of the melting transition [30].

4. Stability assessment of amorphous solid dispersions

In the process of pharmaceutical development, many newly discovered small molecule APIs (~75%) exhibit low aqueous solubility, negatively affecting bioavailability [34,53,54]. Formulation strategies capable of generating supersaturated solutions can address this solubility limitation and increase the absorption of the API. One widely adopted strategy to address these limitations in the aqueous solubility of an API is the formation of multi-component crystalline systems (i.e. co-crystals and salts) [55]. While multi-component systems improve aqueous solubility, these approaches often require further screening efforts to identify new crystal forms amenable to integration into final dosage forms [55]. Small quantities of readily available early-stage material can complicate exhaustive screening efforts. In this context, polarization-dependent SHG measurements have been shown to provide high statistical confidence in crystal form discrimination from measurements of a few μg of material [11].

Another strategy to circumnavigate the identification of amenable multi-component crystals that is finding increasingly rapid adoption in the pharmaceutical industry is through amorphous solid dispersions (ASDs). ASDs are attractive vehicles for increasing dissolution rates and bioavailability for APIs with low aqueous solubility by kinetically trapping API molecules within glassy polymeric matrices with comparatively high aqueous solubility [32,33,56,57]. However, using an ASD increases the susceptibility of a dosage form to physical and chemical degradation relative to crystalline formulations of the API [33,57]. The API dispersed in an ASD often has a higher chemical potential relative to the crystalline state [34,57,58]. This inherent metastability provides a thermodynamic driving force for API crystallization [32], which in turn can then subsequently cause a depletion of the supersaturation (i.e., desupersaturation) and a corresponding loss in bioavailability [59–61]. This thermodynamic driving force is generally tempered by kinetic restrictions on molecular mobility within the glassy matrix of the polymer. The interplay between kinetics and thermodynamics can result in crystal nucleation and growth occurring during both the pharmaceutical manufacturing processes and subsequently upon storage [34,57]. In addition to directly sequestering the API into low bioavailability forms, crystalline API particles can serve as nuclei for desupersaturation upon dissolution, further reducing availability of the solubilized API fraction [33,57]. Monitoring the crystal growth under diverse storage conditions as a function of temperature and humidity can provide predictive tools for quantifying the crystalline fraction and the impact of trace crystallinity on desupersaturation [56,61].

Many questions on the earliest stages of crystal formation are particularly challenging to address due to practical limitations of widely used analytical tools for analysis of crystallization kinetics in ASDs in accelerated stability testing [34]. The earliest stages of crystal formation are critical in reliably determining nucleation and growth kinetics before depletion effects are relevant. In the diffusion-limited growth regime, concentration gradients arising from local depletion can complicate analysis of growth kinetics. Consequently, the earliest stages of crystal growth are least biased by local gradients in API distribution within the polymer matrix and more representative of the native growth kinetics. In addition, onset times for nucleation rate determinations are experimentally biased by an induction time between generation of critical nuclei and their subsequent growth to sizes large enough for detection. For these combined reasons, analytical techniques capable of accessing growth kinetics at these early stages are highly desired. The experimental challenges to be met for trace detection are further exacerbated in ASDs, as the total drug loading is routinely ~10–20% [34,57]. Assessment of the crystalline fraction by pXRD is often limited by x-ray scattering from amorphous material, leading to limits of detection on the order of a few % crystallinity, yielding a total dynamic range of roughly a single order of magnitude [33,56]. Analogous complications arise in vibrational spectroscopic techniques (Raman, near-infrared (NIR) and infrared (IR)), in which background from the amorphous API and polymer increase the lower limits of detection for crystalline forms of the API to a few % crystallinity [57,62]. Many methods [polarized light microscopy (PLM), pXRD, DSC, and solid-state NMR spectroscopy (ssNMR)] are not able to characterize crystallization kinetics *in situ* at storage conditions, as they face limitations of sensitivity when characterizing the API at the representative 10–20% of API drug loading within the ASD [34,56]. While not formally crystal-specific, scanning electron microscopy (SEM) can be used for detection of particles exhibiting crystalline habits, but such assessments of gross morphology lack chemical and solid-state specificity [33]. Furthermore, high resolution generally coincides with a low field of view, such that SEM will necessarily miss trace crystals produced in unsampled locations of the ASD [33]. From this collective assessment, a measurement gap exists between the needs for low crystallinity analysis in ASDs and the relatively high limit of detection available in the most common benchtop methods, largely due to interferences from the background of noncrystalline constituents.

In this context, the near complete rejection of background from non-crystalline materials suggests that SHG (and by extension SFG) may be well suited to address this measurement gap in ASD analysis [57]. Beam-scanning nonlinear optical imaging is inherently confocal, and the focal point can be scanned across the sample horizontally across multiple z-levels which makes rapid 3-dimensional imaging possible [33,53]. SHG images can be acquired over relatively large fields of view (several mm^2) routinely operating at video rate (15–30 frames per second). Under such conditions, crystalline fractions in the ppm regime have been reported, representing a reduction of the lower limits of detection by 2–3 orders of magnitude relative to the common methods described above [56]. As noted previously in the discussion of polymorphism, SHG-guided analysis for background reduction was shown to support reductions in the limits of detection for both Raman and pXRD into similar ppm regimes [57,63]. In addition, most nonlinear optical techniques are non-destructive, supporting repeated measurements over time during pharmaceutical testing [53]. Nonlinear optics provides methods for early detection of crystallization to optimize ASD formulation in storage conditions and processing conditions to improve APIs bioavailability [56,57]. Consistent with these expectations, Sarkar and Song et al. were able to measure crystallization kinetics for APIs *in situ* for early stages of crystallization (<<1%) of ritonavir. Sarkar and Song et al. showed SHG as an analytical tool for accelerated stability testing at low limits of detection (10 ppm), which is 2 orders of magnitude lower than other routine benchtop measurements [34]. In addition, an analytical kinetic model was used with the high sensitivity of SHG in order to predict crystalline fraction, crystalline number density and size distribution, which can lead to characterizations of the oral bioavailability of the API in the ASD. Using a controlled environment for *in situ* stability testing (CEiST) chamber eliminated the need for multiple aliquots of sample typically required for conventional stability tests. The same API crystals were mainatained at 50 °C and 75% relative humidity (RH) over 48 h. Single particle tracking SHG microscopy enabled by CEiST, allowed quantification of the distribution in crystal growth rates

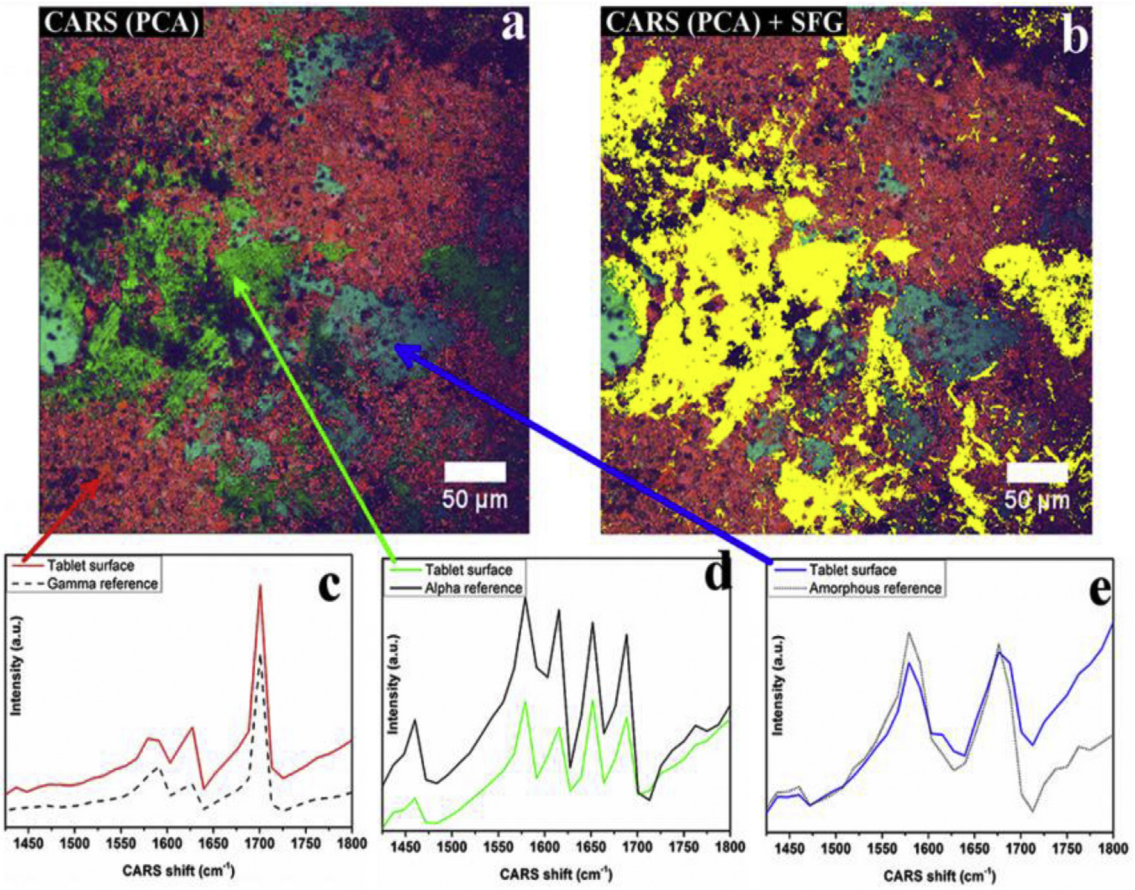

a) The image shows a PCA-based CARS image. In b) the same CARS image (a) is overlaid with the SFG image for the same tablet that contains gamma, alpha and amorphous indomethacin. The CARS spectra is shown from the c) green, d) red, and e) blue regions for the different polymorphic/solid-state form of indometacine. The CARS spectral scan was 1412−1800 cm-1 and the SFG signal was from a 480−490 nm range of wavelengths. Gamma indomethacin can be imaged with CARS at 1701 cm-1, amorphous can be imaged with CARS signal at 1676 cm-1, and alpha indomethacin was observed with SFG/SHG signal (when CARS is not used with the classification PCA) [54].

and greatly improved the SNR in nucleation rate determination for the model drug ritonavir [56].

In addition to all the advantages discussed, multimodal imaging of ASD formulations combining even and odd nonlinear optical effects supports complementary analysis based independently on local symmetry (SHG, SFG), on vibrational spectroscopy (CARS, SRS), and/or on electronic spectroscopy by two-photon excited ultraviolet fluorescence (TPE-UVF). Multimodal nonlinear imaging can support visualization of different solid state forms of APIs, discriminate between crystalline API and crystalline excipients, and simultaneously support imaging of crystalline and amorphous API, as shown in measurements of tadalifil within Cialis™ tablets [64]. Quantification of chemical transformations during stability testing supports the optimization of solid-state forms of drugs in pharmaceutical industry [33,53]. In one notable example, Strachan and coworkers' used a multimodal technique combining nonresonant SFG for probing local symmetry with vibrational-spectroscopic imaging by CARS to monitor amorphous and crystalline alpha and gamma polymorphs of indomethacin during storage. This work appears to be the first combined application of nonlinear imaging techniques to image dynamic phase transformations in pharmaceutical samples. As SFG/SHG imaging is sensitive to non-centrosymmetric crystals, CARS imaging allowed for detection based on molecular vibrations, improving statistical confidence in chemical classification by combined, independent analyses. Strachan and coworkers imaged amorphous indomethacin and the crystalline gamma and alpha forms of indomethacin on the tablet surfaces to gain new insights on the crystallization behavior at low and high humidity. Principal component analysis (PCA) was performed on hyperspectral CARS images sets. Specifically, they found that crystallization (to the gamma form) was more rapid at 23% RH than the crystallization at 75% RH (in the alpha form). In addition, their group showed that the CARS/SFG techniques had higher sensitivity to solid-state crystallization than established, highly used techniques of Raman and FTIR [33].

This example highlights the promise of dimension reduction methods such as PCA and related chemometric analyses to mine nonlinear optical spectroscopic data. Spectral decomposition methods provide a convenient approach for signal to noise enhancement and sample classification [43]. Classic multivariate statistical methods include unsupervised algorithms such as principal component analysis (PCA) and supervised algorithms such as linear discriminant analysis (LDA) and support vector machines (SVM). Unsupervised methods are useful for identifying intrinsic patterns and grouping within complex data sets based on identification of a handful of low-dimensional directions in spectral-space that maximize the total variance within a high-dimensional data set without requiring any prior knowledge. Supervised LDA algorithm leverage classification information within a training set to maximize the resolution between multi-class data sets. SVM is particularly adept at identification of both linear and nonlinear decision boundaries between data sets within a low-dimensional

representation [65]. Although these methods support both signal to noise enhancement and data mining, the nonlinear nature of NLO spectral data can pose unique challenges relative to conventional spectroscopy. Specifically, the linear transformations associated with PCA and LDA implicitly assume that the total signal can be cast as a linear sum of the signals of each component in a multi-component system. However, in nonlinear optics, the *fields* add rather than the intensity. As such, interference effects in the spectral domain (e.g., from a non-resonant background) cannot be properly captured by linear analyses such as PCA and LDA. Extension to nonlinear spectral decomposition approaches such as artificial neural networks for classification or quadratic discriminant analysis for dimension reduction are potentially promising strategies for addressing such complications.

5. Dissolution analysis

Slow dissolution of APIs with low aqueous solubility can negatively affect pharmacokinetics, in turn resulting in reductions in bioavailability. Amorphous solid dispersions can greatly enhance dissolution kinetics through relatively rapid solubilization of the matrix, but the remaining unsolubilized materials can be complex and heterogeneous. Dissolution testing provides an assessment of formulations designed to optimize dissolution kinetics and probe this complexity under conditions that are representative of those expected *in vivo* [32,58]. However, such connections are not trivial. For oral formulations, pH and solution composition can vary widely for dissolution in the gut versus the intestine, as well as for fasted versus fed conditions, complicating *in vitro* estimation of anticipated oral bioavailability [58]. Factors often balanced in evaluating dissolution behaviors of solid dosage forms include the intrinsic solubility of the drug, the overall degree of supersaturation, and the composition/pH of the suspension medium itself. In studies of amorphous solid dispersions, dissolution of the matrix, the degree of supersaturation, and possible phase-separation also affect dissolution behaviors. In addition, preferential loss of the highly soluble fraction in an ASD can produce a low-solubility amorphous skin, further slowing dissolution and complicating kinetics modeling [66–68]. Differences in pH and composition between the stomach and intestinal fluids further complicates predictive modeling. Such complexities are often veiled in dissolution experiments performed by measuring the aqueous-phase concentration alone in simple aqueous media, with corresponding loss in predictive capabilities of *in vivo* performance after oral administration [58,61]. As a consequence of these collective challenges, dissolution experiments performed in simple aqueous media are often poor predictors of *in vivo* performance following oral administration. Access to dissolution information in complex matrices more closely matched to gastrointenstinal fluids representing different environments for absorption may improve both fundamental understanding and quantitative modeling of dissolution kinetics. However, the use of such complex matrices more representative of biological media introduces substantial new measurement challenges [61]. Methods capable of *in vitro* dissolution testing of amorphous API materials in sufficiently complex matrices are needed to build predictive ties to the *in vivo* performance.

There are many conventional methods to connect *in vitro* and *in vivo* dissolution kinetics with unique strengths and limitations for analysis of complex suspensions. HPLC (high performance liquid chromatography) and UV/vis (ultraviolet–visible spectroscopy) are often use to measure the solubilized API fraction in dissolution experiments, but they generally provide little meaningful information on the physiochemical changes of the drug or matrix in the condensed state to assess compositional changes within the dissolving compact [69]. Conventional approaches for IR, Raman, and mass spectrometric imaging (MSI) were used for drug dissolution experiments, but have their own sets of limitations [32,69]. IR spectroscopy suffers from high attenuation from water absorption, limiting its use for aqueous dissolution media. Spontaneous Raman imaging is limited due to long image acquisition times [32,69]. Although MS has moderate spatial resolution (10–100 μm) and high chemical specificity, the buried interfaces driving dissolution are challenging to access by conventional MS sampling methods [69]. Solid-state analysis with dissolution testing has been attempted to understand the surface solid-state phenomena affecting the dissolution process, with the main analytical instruments used in these studies being PLM and attenuated total reflectance-FTIR (ATR-FTIR). However, PLM has limited solid-state specificity, and water complicates ATR-FTIR analysis [32]. Clearly, new and complementary methods capable of rapidly and selectively informing on molecular composition non-destructively with high spatial and temporal resolution could potentially address lingering questions regarding dissolution processes.

Nonlinear optical microscopy provides an avenue to address this gap to connect *in vivo* performance with *in vitro* dissolution studies. NLO methods offer rapid contactless sampling with submicron resolution and high sensitivity to composition based on symmetry and/or spectroscopy. In addition, NLO imaging methods can detect crystallization earlier than the aforementioned competing methods without limitations due to water [32]. Recent advances that apply several complementary nonlinear optical measurements to dissolution show the applicability and effectiveness of these techniques, as discussed below.

SHG and two photon excitation-ultraviolet fluorescence (TPE-UVF) of ezemtimibe can support evaluation of drug release mechanics, supersaturation and crystallization kinetics in *in vivo* fasted-state biorelevant media representing both the gastric and intestinal conditions, as shown by Elkhabaz et al. and highlighted in Fig. 3 [70]. Dissolution rates of ezemtimibe ASDs by SHG and TPE-UVF provided evidence for supersaturation and losses from subsequent API crystallization within biomimetic fluids representative of the intestinal compartments (e.g., Ensure™ Plus solutions for gastric compartment). Despite the turbidity and chemical complexity of the dissolution matrices, SHG was able to selectively detection trace crystallization 30 min after initiation of dissolution. Subsequent SHG microscopy measurements revealed the presence of crystals during the gastric stage of dissolution for both media systems and increase of crystallization from seeded crystals in the intestinal stage for low drug loadings (10 and 25%) [70]. The appearance of crystallization coincided with the onset of desupersaturation, implicating solid state phase transformation as a potential API loss mechanism following gastrointenstinal solubilization. These result lay a foundation for broader application of SHG in dissolution testing to connect *in vivo* processes and *in vitro* experiments [58].

Complementing this prior work by SHG and TPE-UVF imaging, SRS microscopy has enabled measurements and modeling of topical drug delivery systems (DDSs) [69]. Motivated by the failure of bulk analysis to monitor dynamic processes (matrix swelling, drug degradation and diffusion), Francis et al. recently implemented SRS for *in situ* dissolution testing of two DDS polymers to provide accurate dissolution kinetics for improved modeling. Although SRS has been used before for static chemical mapping of drugs and excipients in final dosage forms [71], Francis et al. showed that SRS allowed for greater visualization of both drug formulation and single particle tracking dissolution when compared to previously *in situ* measurements by CARS due to SRS's absence of a non-resonant background and its linear scaling with

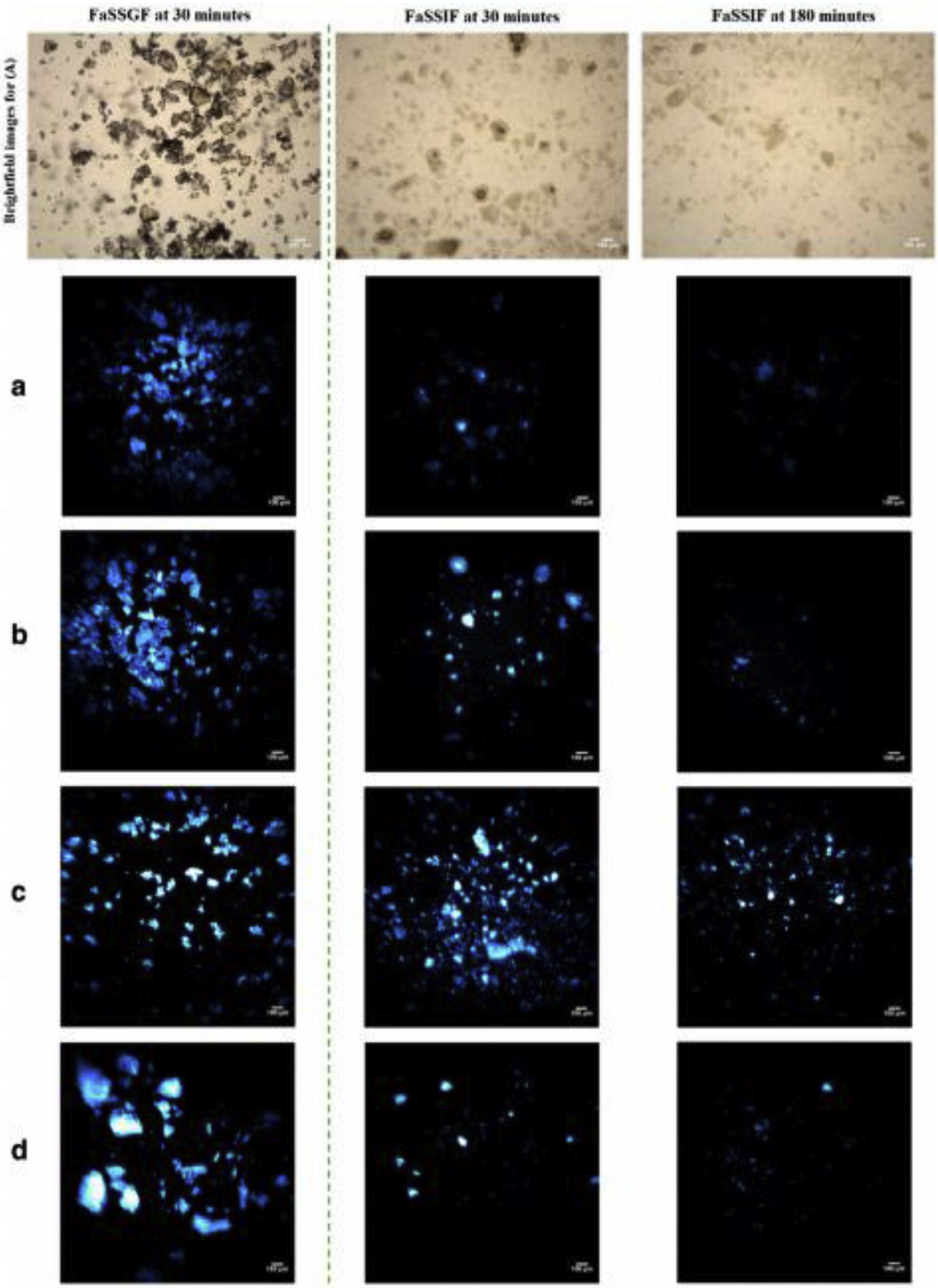

Fig. 3. Bright-field and TPE-UVF images reproduced from Elkhabaz et al. (2019), where SHG and TPE-UVF were used to measure the onset of dissolution of posaconazole ASDs. Although SHG differentiated the chiral crystals from the disordered amorphous background, TPE-UVF acted as a complement to detect posaconozole irrespective of physical state. Brightfield images of the posaconazole ASDs are shown on top in dissolution in FaSSGF at 30 min (fasted-state simulated gastric fluid) and FaSSIF (fasted-state simulated intestinal fluid) at 30 and 180 min. TPE-UVF images are shown for the same conditions for (a) 10%, (b) 25%, and (c) 50% drug loading with (d) being the tablet powder in dissolution. As these are TPE-UVF images, the blue is the undissolved posaconazole (either crystallized or undissolved ASD). The scale bar in the images is 100 micrometers.

chemical concentration [69]. *In situ* dissolution measured by SRS was used to calculate the percent volume loss of 39 individual particles, which would have been difficult quantitatively by CARS due to its non-resonant background. In addition, SRS enabled single particle tracking measurements during dissolution that correlated with UV/vis spectroscopy performed in the solution in contact with the same particle area. Interestingly, Francis et al. showed through particle tracking that dissolution kinetics were independent of both particle size and depth [69]. With the improvement of *in situ* dissolution testing with SRS, *in vitro* experiments can support improved prediction of *in vivo* performance through understanding of spatially resolved transformations, in turn informing pharmacokinetic modeling for better prediction of drug release.

6. Conclusion

Nonlinear optical methods for drug formulation analysis were shown to improve testing times for polymorphic determination, formulation, stability and dissolution testing. NLO methods provide rapid, nondestructive analysis with low sample size requirements. As the cost of ultrafast laser sources continues to decline (e.g., through availability of ultrafast fiber lasers), NLO methods are likely to become increasingly available for widespread integration into pharmaceutical formulations analysis pipelines. This review is designed to provide a current snapshot of the unique information content accessible through nonlinear optical imaging and analysis. As these fields continue to progress and novel NLO methods arise, it is clear that NLOs will play an increasingly important role supporting drug discovery and testing.

Given the numerous advantages of nonlinear optical imaging methods for multiple critical aspects of pharmaceutical analysis, the pace of industrial adoption has arguably not matched the pace of scientific discovery. Several barriers complicating broad adoption by the pharmaceutical community may be driving these trends. First, there is a perception that ultrafast laser sources commonly used for NLO microscopy can be prohibitively expensive and complex. This was certainly true a decade ago, when ultrafast solid-state lasers were confined primarily to specialized optics research laboratories. However, the recent emergence of turnkey and affordable ultrafast fiber lasers has opened access to ultrafast optics with price-points comparable to conventional cw laser sources commonly used in confocal microscopy. The recent availability of turn-key commercial instrumentation for SHG and TPE-UVF microscopy analysis of pharmaceutical powders (Formulatrix) has the potential to accelerate broader access. Automated image analysis algorithms support calibration-free quantitation of crystal fraction over a large dynamic range [72], further lowering the barriers for broader adoption.

Another perceptual barrier for broad adoption may rest with a validation conundrum; if SHG microscopy can detect crystallinity with limits of detection many orders of magnitude lower than other commercially available instruments, how does one independently validate the results obtained by SHG within this regime? Efforts to address this issue have demonstrated the use of SHG imaging to guide targeted independent characterization by both Raman spectroscopy [38,63] and by localized synchrotron X-ray diffraction [73], with the guided analysis enabling independent confirmation of composition with limits of detection similar to SHG imaging (e.g. parts per million crystalline content).

Finally, adoption of nonlinear optical methods may also be slowed by a general risk-aversion to new technologies within the pharmaceutical research community. Unlike other scientific research areas, final dosage forms of pharmaceutical products are designed and manufactured within strict regulatory environments. Using emerging methods that do not have extensive histories of vetting can potentially introduce risks; new information emerging on the instrumental approach itself may potentially require re-interpretation of prior measurements. Early-stage discovery has considerably greater latitude, but can still reflect some of this inherent cautiousness. As the body of research in both academic and industrial settings continues to grow, the strengths and limitations of the methods continues to become more completely mapped, lowering risks for broad adoption.

Declaration of competing interest

The authors declare no conflict of interest.

Acknowledgements

The authors acknowledge the support from the NSF (GOALI:CDS&E #1710475, I/UCRC #1916691, and CIF #1763896).

References

[1] G.A. Van Norman, Drugs, devices, and the FDA: Part 1: an overview of approval processes for drugs, JACC (J. Am. Coll. Cardiol.) 1 (3) (2016) 170–179. Basic to Translational Science.
[2] X.Y. Lawrence, Pharmaceutical quality by design: product and process development, understanding, and control, Pharm. Res. (N. Y.) 25 (4) (2008) 781–791.
[3] L.X. Yu, Pharmaceutical quality by design: product and process development, understanding, and control, Pharmaceut. Res. 25 (4) (2008) 781–791.
[4] K.M. Hanson, C.J. Bardeen, Application of nonlinear optical microscopy for imaging skin, Photochem. Photobiol. 85 (1) (2009) 33–44.
[5] G.J. Simpson, Nonlinear Optical Polarization Analysis in Chemistry and Biology, Cambridge Univ Press, Cambridge, 2017, pp. 1–485.
[6] R.W. Boyd, Nonlinear Optics, third ed., Elsevier Academic Press Inc, San Diego, 2008, pp. 1–613.
[7] Y.-R. Shen, The Principles of Nonlinear Optics, Wiley-Interscience, New York, 1984.
[8] A.J. Moad, G.J. Simpson, A unified treatment of selection rules and symmetry relations for sum-frequency and second harmonic spectroscopies, J. Phys. Chem. B 108 (11) (2004) 3548–3562.
[9] M.C. Nunez, M.E. Garcia-Rubino, A. Conejo-Garcia, O. Cruz-Lopez, M. Kimatrai, M.A. Gallo, A. Espinosa, J.M. Campos, Homochiral drugs: a demanding tendency of the pharmaceutical industry, Curr. Med. Chem. 16 (16) (2009) 2064–2074.
[10] L.M. Haupert, G.J. Simpson, Chirality in nonlinear optics, Annu. Rev. Phys. Chem. 60 (2009) 345–365.
[11] P.D. Schmitt, E.L. DeWalt, X.Y. Dow, G.J. Simpson, Rapid discrimination of polymorphic crystal forms by nonlinear optical Stokes ellipsometric microscopy, Anal. Chem. 88 (11) (2016) 5760–5768.
[12] S.Z. Sullivan, E.L. DeWalt, P.D. Schmitt, R.M. Muir, G.J. Simpson, Synchronous-digitization for video rate polarization modulated beam scanning second harmonic generation microscopy, in: T.G. Brown, C.J. Cogswell, T. Wilson (Editors), Three-Dimensional and Multidimensional Microscopy: Image Acquisition and Processing Xxii vol. 9330, Spie-Int Soc Optical Engineering, Bellingham, 2015.
[13] X.Y. Dow, E.L. DeWalt, S.Z. Sullivan, P.D. Schmitt, J.R.W. Ulcickas, G.J. Simpson, Imaging the nonlinear susceptibility tensor of collagen by nonlinear optical Stokes ellipsometry, Biophys. J. 111 (7) (2016) 1361–1374.
[14] J.R. Ulcickas, C. Ding, F. Deng, G.J. Simpson, Spatially encoded polarization-dependent nonlinear optics, Optic Lett. 43 (24) (2018) 5973–5976.
[15] D. Singhal, W. Curatolo, Drug polymorphism and dosage form design: a practical perspective, Adv. Drug Deliv. Rev. 56 (3) (2004) 335–347.
[16] B.G. Pereira, F.D. Fonte-Boa, J. Resende, C.B. Pinheiro, N.G. Fernandes, M.I. Yoshida, C.D. Vianna-Soares, Pseudopolymorphs and intrinsic dissolution of nevirapine, Cryst. Growth Des. 7 (10) (2007) 2016–2023.
[17] A.J. Aguiar, J.E. Zelmer, Dissolution behavior of polymorphs of chloramphenicol palmitate and mefenamic acid, J. Pharmaceut. Sci. 58 (8) (1969) 983–+.
[18] J. Bauer, S. Spanton, R. Henry, J. Quick, W. Dziki, W. Porter, J. Morris, Ritonavir: an extraordinary example of conformational polymorphism, Pharm. Res. (N. Y.) 18 (6) (2001) 859–866.
[19] P. Lang, V. Kiss, R. Ambrus, G. Farkas, P. Szabo-Revesz, Z. Aigner, E. Varkonyi, Polymorph screening of an active material, J. Pharmaceut. Biomed. Anal. 84 (2013) 177–183.
[20] J.A. Zeitler, K. Kogermann, J. Rantanen, T. Rades, P.F. Taday, M. Pepper, J. Aaltonen, C.J. Strachan, Drug hydrate systems and dehydration processes studied by terahertz pulsed spectroscopy, Int. J. Pharm. 334 (1–2) (2007) 78–84.

[21] C.J. Strachan, T. Rades, K.C. Gordon, J. Rantanen, Raman spectroscopy for quantitative analysis of pharmaceutical solids, J. Pharm. Pharmacol. 59 (2) (2007) 179–192.
[22] S. Cherukuvada, A. Nangia, Polymorphism in an API ionic liquid: ethambutol dibenzoate trimorphs, CrystEngComm 14 (23) (2012) 7840–7843.
[23] D. Giron, Thermal-analysis and calorimetric methods in the characterization of polymorphs and solvates, Thermochim. Acta 248 (1995) 1–59.
[24] M.R. Caira, Polymorphism vol. 5, Elsevier Science Bv, Amsterdam, 2008, pp. 597–629.
[25] P.D. Schmitt, Recent advances in nonlinear optical analyses of pharmaceutical materials in the solid state, Mol. Pharm. 14 (3) (2017) 555–565.
[26] M. Shevlin, Practical high-throughput experimentation for chemists, ACS Med. Chem. Lett. 8 (6) (2017) 601–607.
[27] S.L. Monissette, O. Almarsson, M.L. Peterson, J.F. Remenar, M.J. Read, A.V. Lemmo, S. Ellis, M.J. Cima, C.R. Gardner, High-throughput crystallization: polymorphs, salts, co-crystals and solvates of pharmaceutical solids, Adv. Drug Deliv. Rev. 56 (3) (2004) 275–300.
[28] G.B. Fogazzi, J. Delanghe, Microscopic examination of urine sediment: phase contrast versus bright field, Clin. Chim. Acta 487 (2018) 168–173.
[29] M. Alhijjaj, M. Reading, P. Belton, S. Qi, Thermal analysis by structural characterization as a method for assessing heterogeneity in complex solid pharmaceutical dosage forms, Anal. Chem. 87 (21) (2015) 10848–10855.
[30] A.M. Sherman, A.C. Geiger, C.J. Smith, L.S. Taylor, J. Hinds, P.A. Stroud, G.J. Simpson, Stochastic differential scanning calorimetry by nonlinear optical microscopy, Anal. Chem. 92 (1) (2020) 1171–1178.
[31] D. Meza-Figueroa, M. Barboza-Flores, F.M. Romero, M. Acosta-Elias, E. Hernandez-Mendiola, F. Maldonado-Escalante, E. Perez-Segura, B. Gonzalez-Grijalva, M. Meza-Montenegro, L. Garcia-Rico, S. Navarro-Espinoza, K. Santacruz-Gomez, A. Gallego-Hernandez, M. Pedroza-Montero, Metal bioaccessibility, particle size distribution and polydispersity of playground dust in synthetic lysosomal fluids, Sci. Total Environ. 713 (2020) 12.
[32] D. Novakovic, A. Isomaki, B. Pleunis, S.J. Fraser-Miller, L. Peltonen, T. Laaksonen, C.J. Strachan, Understanding dissolution and crystallization with imaging: a surface point of view, Mol. Pharm. 15 (11) (2018) 5361–5373.
[33] D. Novakovic, J. Saarinen, T. Rojalin, O. Antikainen, S.J. Fraser-Miller, T. Laaksonen, L. Peltonen, A. Isomaki, C.J. Strachan, Multimodal nonlinear optical imaging for sensitive detection of multiple pharmaceutical solid-state forms and surface transformations, Anal. Chem. 89 (21) (2017) 11460–11467.
[34] Z.T. Song, S. Sarkar, A.D. Vogt, G.D. Danzer, C.J. Smith, E.J. Gualtier, G.J. Simpson, Kinetic modeling of accelerated stability testing enabled by second harmonic generation microscopy, Anal. Chem. 90 (7) (2018) 4406–4413.
[35] B. Sarri, R. Canonge, X. Audier, V. Lavastre, G. Penarier, J. Alie, H. Rigneault, Discriminating polymorph distributions in pharmaceutical tablets using stimulated Raman scattering microscopy, J. Raman Spectrosc. 50 (12) (2019) 1896–1904.
[36] J.G. Porquez, A.D. Slepkov, Application of spectral-focusing-CARS microscopy to pharmaceutical sample analysis, AIP Adv. 8 (9) (2018) 7.
[37] B. Lu, S.Y. Liu, D.P. Yan, Recent advances in photofunctional polymorphs of molecular materials, Chin. Chem. Lett. 30 (11) (2019) 1908–1922.
[38] A.U. Chowdhury, D.H. Ye, Z.T. Song, S.J. Zhang, H.G. Hedderich, B. Mallick, S. Thirunahari, S. Ramakrishnan, A. Sengupta, E.J. Gualtieri, C.A. Bouman, G.J. Simpson, Second harmonic generation guided Raman spectroscopy for sensitive detection of polymorph transitions, Anal. Chem. 89 (11) (2017) 5959–5966.
[39] T.Y. Chang, Q.J. Guo, L.Y. Liu, H.L. Cui, Nondestructive thickness inspection of capsule coating by terahertz time-domain spectroscopy, Ieee Transactions on Terahertz Science and Technology 8 (6) (2018) 688–695.
[40] M. Ito, R. Tokuda, H. Suzuki, T. Sakamoto, K. Terada, S. Noguchi, Desolvation behavior of indinavir sulfate ethanol and follow-up by terahertz spectroscopy, Int. J. Pharm. 567 (2019) 7.
[41] V.H. da Silva, F.S. Vieira, J.J.R. Rohwedder, C. Pasquini, C.F. Pereira, Multivariate quantification of mebendazole polymorphs by terahertz time domain spectroscopy (THZ-TDS), Analyst 142 (9) (2017) 1519–1524.
[42] N.R. Rexrode, J. Orien, M.D. King, Effects of solvent stabilization on pharmaceutical crystallization: investigating conformational polymorphism of probucol using combined solid-state density functional theory, molecular dynamics, and terahertz spectroscopy, J. Phys. Chem. 123 (32) (2019) 6937–6947.
[43] N.L. Calvo, R.M. Maggio, T.S. Kaufman, Chemometrics-assisted solid-state characterization of pharmaceutically relevant materials. Polymorphic substances, J. Pharmaceut. Biomed. Anal. 147 (2018) 518–537.
[44] A.R. Pallipurath, F. Civati, J. Sibik, C. Crowley, J.A. Zeitler, P. McArdle, A. Erxleben, A comprehensive spectroscopic study of the polymorphs of diflunisal and their phase transformations, Int. J. Pharm. 528 (1–2) (2017) 312–321.
[45] M.T. Ruggiero, J.J. Sutton, S.J. Fraser-Miller, A.J. Zaczek, T.M. Korter, K.C. Gordon, J.A. Zeitler, Revisiting the thermodynamic stability of indomethacin polymorphs with low-frequency vibrational spectroscopy and quantum mechanical simulations, Cryst. Growth Des. 18 (11) (2018) 6513–6520.
[46] S. Warnecke, J.X. Wu, A. Rinnan, M. Alleso, F. van den Berg, P.U. Jepsen, S.B. Engelsen, Quantifying crystalline a-lactose monohydrate in amorphous lactose using terahertz time domain spectroscopy and near infrared spectroscopy, Vib. Spectrosc. 102 (2019) 39–46.
[47] P. Bawuah, D. Markl, D. Farrell, M. Evans, A. Portieri, A. Anderson, D. Goodwin, R. Lucas, J.A. Zeitler, Terahertz-based porosity measurement of pharmaceutical tablets: a tutorial, J. Infrared, Millim. Terahertz Waves 41 (4) (2020) 450–469.
[48] S.Z. Sullivan, R.D. Muir, J.A. Newman, M.S. Carlsen, S. Sreehari, C. Doerge, N.J. Begue, R.M. Everly, C.A. Bouman, G.J. Simpson, High frame-rate multichannel beam-scanning microscopy based on Lissajous trajectories, Optic Express 22 (20) (2014) 24224–24234.
[49] B. Wunderlich, Theory of cold crrystallization of high polymers, J. Chem. Phys. 29 (6) (1958) 1395–1404.
[50] D.A. Turton, H.M. Senn, T. Harwood, A.J. Lapthorn, E.M. Ellis, K. Wynne, Terahertz underdamped vibrational motion governs protein-ligand binding in solution, Nat. Commun. 5 (1) (2014) 3999.
[51] C.V. Berney, V. Renugopalakrishnan, R.S. Bhatnagar, Collagen. An inelastic neutron-scattering study of low-frequency vibrational modes, Biophys. J. 52 (2) (1987) 343–345.
[52] L.Q. Ren, I. Hurwitz, D. Raanan, P. Oulevey, D. Oron, Y. Silberberg, Terahertz coherent anti-Stokes Raman scattering microscopy, Optica 6 (1) (2019) 52–55.
[53] R. Ojarinta, J. Saarinen, C.J. Strachan, O. Korhonen, R. Laitinen, Preparation and characterization of multi-component tablets containing co-amorphous salts: combining multimodal non-linear optical imaging with established analytical methods, Eur. J. Pharm. Biopharm. 132 (2018) 112–126.
[54] P.T. Mah, D. Novakovic, J. Saarinen, S. Van Landeghem, L. Peltonen, T. Laaksonen, A. Isomäki, C.J. Strachan, Elucidation of compression-induced surface crystallization in amorphous tablets using sum frequency generation (SFG) microscopy, Pharmaceut. Res. 34 (5) (2017) 957–970.
[55] D.P. Elder, R. Holm, H.L. de Diego, Use of pharmaceutical salts and cocrystals to address the issue of poor solubility, Int. J. Pharm. 453 (1) (2013) 88–100.
[56] S. Sarkar, Z. Song, S.R. Griffin, N. Takanti, A.D. Vogt, A. Ruggles, G.D. Danzer, G.J. Simpson, In situ crystal growth rate distributions of active pharmaceutical ingredients, Mol. Pharm. 17 (3) (2020) 769–776.
[57] C. Correa-Soto, N.S. Trasi, P.D. Schmitt, Y. Su, Z. Liu, E. Miller, N. Variankaval, P.J. Marsac, G.J. Simpson, L.S. Taylor, Second harmonic generation microscopy as a tool for the early detection of crystallization in spray dried dispersions, J. Pharmaceut. Biomed. Anal. 146 (2017) 86–95.
[58] A. Elkhabaz, S. Sarkar, G.J. Simpson, L.S. Taylor, Characterization of phase transformations for amorphous solid dispersions of a weakly basic drug upon dissolution in biorelevant media, Pharmaceut. Res. 36 (12) (2019) 174.
[59] U.K. Singh, M.A. Pietz, M.E. Kopach, Identifying scale sensitivity for API crystallizations from desupersaturation measurements, Org. Process Res. Dev. 13 (2) (2009) 276–279.
[60] Y. Hu, J.K. Liang, A.S. Myerson, L.S. Taylor, Crystallization monitoring by Raman Spectroscopy: simultaneous measurement of desupersaturation profile and polymorphic form in flufenamic acid systems, Ind. Eng. Chem. Res. 44 (5) (2005) 1233–1240.
[61] A. Elkhabaz, S. Sarkar, J.K. Dinh, G.J. Simpson, L.S. Taylor, Variation in supersaturation and phase behavior of ezetimibe amorphous solid dispersions upon dissolution in different biorelevant media, Mol. Pharm. 15 (1) (2018) 193–206.
[62] L. Ilium, Chitosan and its use as a pharmaceutical excipient, Pharmaceut. Res. 15 (9) (1998) 1326–1331.
[63] P.D. Schmitt, N.S. Trasi, L.S. Taylor, G.J. Simpson, Finding the needle in the haystack: characterization of trace crystallinity in a commercial formulation of paclitaxel protein-bound particles by Raman spectroscopy enabled by second harmonic generation microscopy, Mol. Pharm. 12 (7) (2015) 2378–2383.
[64] S. Toth, J. Madden, L. Taylor, P. Marsac, G. Simpson, Selective imaging of active pharmaceutical ingredients in powdered blends with common excipients utilizing two-photon excited ultraviolet-fluorescence and ultraviolet-second order nonlinear optical imaging of chiral crystals, Anal. Chem. 84 (14) (2012) 5869–5875.
[65] K.J.I. Ember, M.A. Hoeve, S.L. McAughtrie, M.S. Bergholt, B.J. Dwyer, M.M. Stevens, K. Faulds, S.J. Forbes, C.J. Campbell, Raman spectroscopy and regenerative medicine: a review, npj Regenerative Medicine 2 (1) (2017) 12.
[66] A. Singh, G. Van den Mooter, Spray drying formulation of amorphous solid dispersions, Adv. Drug Deliv. Rev. 100 (2016) 27–50.
[67] A. Haser, F. Zhang, New strategies for improving the development and performance of amorphous solid dispersions, AAPS PharmSciTech 19 (3) (2018) 978–990.
[68] M. Kennedy, J. Hu, P. Gao, L. Li, A. Ali-Reynolds, B. Chal, V. Gupta, C. Ma, N. Mahajan, A. Akrami, Enhanced bioavailability of a poorly soluble VR1 antagonist using an amorphous solid dispersion approach: a case study, Mol. Pharm. 5 (6) (2008) 981–993.
[69] A.T. Francis, T.T. Nguyen, M.S. Lamm, R. Teller, S.P. Forster, W. Xu, T. Rhodes, R.L. Smith, J. Kuiper, Y. Su, D. Fu, In situ stimulated Raman scattering (SRS) microscopy study of the dissolution of sustained-release implant formulation, Mol. Pharm. 15 (12) (2018) 5793–5801.
[70] A. Elkhabaz, S. Sarkar, G.J. Simpson, L.S. Taylor, Characterization of phase transformations for amorphous solid dispersions of a weakly basic drug upon dissolution in biorelevant media, Pharm. Res. (N. Y.) 36 (12) (2019) 17.

[71] M.N. Slipchenko, H. Chen, D.R. Ely, Y. Jung, M.T. Carvajal, J.-X. Cheng, Vibrational imaging of tablets by epi-detected stimulated Raman scattering microscopy, Analyst 135 (10) (2010) 2613–2619.
[72] C.J. Smith, J. Dinh, P.D. Schmitt, P.A. Stroud, J. Hinds, M.J. Johnson, G.J. Simpson, Calibration-free second harmonic generation (SHG) image analysis for quantification of trace crystallinity within final dosage forms of amorphous solid dispersions, Appl. Spectrosc. 72 (11) (2018) 1594–1605.
[73] J.A. Newman, P.D. Schmitt, S.J. Toth, F.Y. Deng, S.J. Zhang, G.J. Simpson, Parts per million powder X-ray diffraction, Anal. Chem. 87 (21) (2015) 10950–10955.